A first step towards moving metasurfaces with microwaves : a spinning Split Ring Resonator experiment

Côme Jodet, Olivier Pascal, Jérôme Sokoloff

A first step towards moving metasurfaces with microwaves : a spinning Split Ring Resonator experiment

Côme Jodet*
LAPLACE, Université de Toulouse, CNRS, INPT, UPS, Toulouse, France and Anywaves, 2 Esplanade Compans Caffarelli, 31000 Toulouse, France

Olivier Pascal and Jérôme Sokoloff
LAPLACE, Université de Toulouse, CNRS, INPT, UPS, Toulouse, France
(Dated: July 30, 2023)

The long term goal is to set metasurfaces in motion using microwaves. As a first step, this work focuses on a single usual element, the Split Ring Resonator (SRR). A method is established, and its application to the SRR case leads to the use of a circularly polarized wave. Analytical, numerical and experimental studies carried out confirm that a circular polarized wave can set a SRR in rotation. Thus, at 2.45GHz, for 150W, the 15mm-diameter SRR was rotated over several rotations and reached speeds of the order of 0.5 rps. The limits and possibilities of this initial work are discussed.

Electromagnetic waves are mainly used to carry information, notably in telecommunications. The energy or power they also carry is mainly used for heating, as in microwave ovens. However, electromagnetic waves can, even in the slightest way, set in motion an object with which they interact.

This interaction can be approached as a momentum transfer. These transfers have been observed, theorized and then measured experimentally. In 1619, while observing the tails of comets, which always point away from the sun, Kepler intuited the existence of a "solar wind" [1]. This phenomenon is theorized by Maxwell more than two centuries later, introducing the notion of linear momentum of the electromagnetic wave [2]. The latter can therefore exert pressure on a surface it illuminates. The first measurements of this property were made independently by Lebedew [3] and Nichols and Hull in 1901 [4,5]. The angular momentum (AM) of an electromagnetic wave (and therefore its ability to rotate an object) is theorized by Poynting in 1909. [6]. The AM can be separated into two parts, one corresponding to the spin angular momentum (SAM) related to the circular polarization of light, and the other to the orbital angular momentum (OAM) of the wave.

The experimental demonstrations of the existence of the AM have been carried out by measuring his transfer to a material object. Concerning SAM, it has been initiated by Beth in 1935 [7,8] and Holbourn [9] in the optical range, followed by Allen in 1966 [10] in the microwave range (whose work was later sharpened by Kristensen in 1994 [11]). The first direct measurement of transfer to a macroscopic object was carried out by Delannoy in 2004 [12]. For the OAM, it has been carried out by He in 1994 [13] in the field of optics, then by Emile in 2014 in the microwave field [14]. As a result of these pioneering works, all the components of the *momentum* have been demonstrated experimentally, in both the optical and microwave ranges.

In complement to these experimental demonstrations of wave momentum transfer, the exploitation of the mechanical properties of the wave opens up multiple fields of application [15]. In optics, it is used for trapping [16] and cooling [17] of atoms, as well as for the controlling molecules and micrometric particles [18]. The AM of the wave adds new degrees of freedom in these areas [19], and could, for example, enable gyroscopic control of micrometric particles [20]. On a macroscopic scale, the rotational Doppler effect can be used to measure the rotation speed of macroscopic objects [21] and *solar sails* are an application of linear momentum exploitation [22, 23].

The use of metasurfaces and the electromagnetic properties they can provide allows broad applications to be envisaged [24]. Their implementation in the microwave range offers various advantages. One is that sustained high power is currently easier to obtain in this frequency range. Another is that, since the wavelength is in the centimetre range, the elements composing these metasurfaces are macroscopic. These elements, and hence the metasurfaces, are therefore easier to shape. Finally, at this scale, electrical quantities such as charges and currents in the elements, as well as the exploitation of resonance, make it easier to envisage sizing to generate motion via the Lorentz force.

Consequently, it has been chosen not to continue with the historic momentum transfer approach. Instead, a classical electrodynamic approach is adopted, as synthesized by Jackson [25] or Griffith [26], and deepened by Mansuripur [27]. This vision describes the interactions between the electromagnetic wave - represented by the **E** and **H** fields - and matter - represented by the charge density ρ and the current density **J** within it -. With the aim of setting an object in motion with an electromagnetic field, this choice enables us to envisage complex behaviours and interactions [24].

As a first approach, the focus here is solely on a single element of the metasurface. In order to exploit the

* come.jodet@laplace.univ-tlse.fr

interactions and resonance phenomena mentioned above, the Split Ring Resonator (SRR) is chosen. Introduced by Pendry *et al.* [28], SRR are often used as building blocks of metamaterials enabling negative permittivity and permeability media [29, 30], opening up a wide field of research [31, 32].

A device designed to rotate an SRR using an electromagnetic wave at microwave frequencies, is built. Analytical and numerical approaches are carried out, then experimental implementation is performed and discussed. To the authors' knowledge, no such approach has ever been published. The device presented is an example of what this approach can allow, and a first step towards an application with metasurfaces.

Method, application and modeling - The aim is to rotate a SRR using an electromagnetic field. As such an approach is not yet covered in the literature, a method has been established. This method is broader than the SRR case discussed in this letter. Several data have to be considered as input to address this issue : the type of element (here the SRR), the nature of the source (here an electromagnetic wave), the kind of force (here a torque). In this case, the use of resonance to intensify the desired torque is added. From these initial choices, the method consists of three parallel stages. One is to specify the properties of the electromagnetic quantities and the element to cover all the initial choices, insofar as possible. Another is to spatially organize the electromagnetic quantities (here the magnetic field $\mathbf{H}$ and the current density $\mathbf{J}$) to obtain the desired resultant force. A third is to temporally organize these same electromagnetic quantities, in order to obtain a non-zero time-averaged force. What results is a spatio-temporal arrangement of electromagnetic fields and materials that (if possible) delivers the desired force.

For the application discussed in this letter, the method and initial choices described above lead to the device shown in figure 1. The choice of SRR and wave implies the use of induction and Laplace force, that are related to the vector product $\mathbf{J} \times \mu_0 \mathbf{H}$. The SRR is resonant and inductive by design, which validates the first step. Spatially, the organization of $\mathbf{J}$ is imposed by the SRR (here the first resonance mode is considered as depicted in figure 1a). For the $\mathbf{H}$ field, a component $\mathbf{H}_\perp$ normal to the SRR surface (see fig. 1a) is required to induce a current in it. To obtain maximum average torque for a given power, another tangential component is required. By symmetry of the system, we choose the axis of rotation to pass through the center of the SRR and through the center of its gap (Δ axis, see fig. 1a). This determines the tangential component $\mathbf{H}_\parallel$ (see fig. 1a). Temporally, according to Lenz's law, the induced current is in phase quadrature compared to the inductive field $\mathbf{H}_\perp$. $\mathbf{H}_\parallel$ has to be in phase with the current to obtain a non-zero time-averaged force, meaning that $\mathbf{H}_\parallel$ has to be in the same phase quadrature compared to $\mathbf{H}_\perp$. Overall, the method leads thus to the use of a circularly polarized wave to rotate an SRR (see fig 1). In this way, the system becomes invariant to SRR rotation, which is in line with the desired motion.

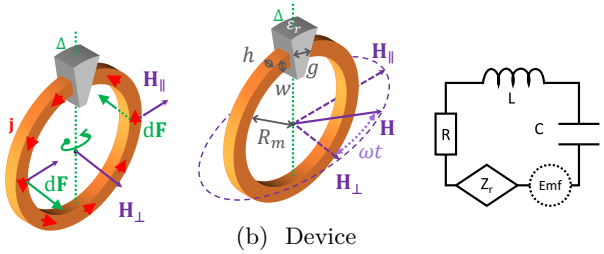

(a) Principe of torque generation. (b) Device parameterization (SRR + field). (c) SRR equivalent circuit.

FIG. 1: Device modeling.

A simple analytical model of the resulting device can be drawn up (Figure 1). The SRR is likened to an electrical circuit composed of an inductor L in serie with a capacitor C, a resistor R modeling the material's resistivity, and an impedance Z_r modeling the SRR's high-frequency radiation. The electromotive force (Emf) models current induction. To adjust the resonant frequency (via the value of C), a dielectric is added to the gap. Considering the powers involved ($> 100W$), this also helps to prevent breakdown in the gap, where the electric field is particularly intense.

Working at resonance, an approximate formulation is established for the current $i_{res}(t)$ induced in the SRR, given by equation (1). It then gives the resulting time average torque $\langle \Gamma_{res} \rangle$, the amplitude of which is given by equation (2). Neglecting all friction and restoring torques, the time average rotation acceleration $\langle \alpha_{res} \rangle$ of the SRR is deducted, as given by equation (3).

$$i_{res}(t) = \frac{\pi R_m^2 \ \mu_0 H_{0,\perp}}{(R + Z_r)\sqrt{LC}} \sin\left(\frac{1}{\sqrt{LC}}\ t\right) \tag{1}$$

$$\langle \Gamma_{res} \rangle = \frac{1}{2} \frac{(\pi R_m^2)^2 \mu_0^2 H_{0,\perp} H_{0,\parallel}}{(R + Z_r)\sqrt{LC}} \tag{2}$$

$$\langle \alpha_{res} \rangle = \frac{\langle \Gamma_{res} \rangle}{J_\Delta} \tag{3}$$

R_m is the mean radius of the SRR, $H_{0,\perp}$ and $H_{0,\parallel}$ are respectively the magnitude of the normal $\mathbf{H}_\perp$ and tangential $\mathbf{H}_\parallel$ components of the magnetic field and J_Δ is the moment of inertia of the SRR. Supplementary materials provide further details of the analytical modeling carried out.

In order to build an experimental prototype, the resonant frequency of the SRR (and therefore that of the incident field) is set at 2.45GHz and a set of parameters suitable for a copper SRR is deduced [33,34] ($R_m = 7.5mm$, $g = 1mm$, $h = w = 1mm$, $\epsilon_r = 3.27$). With these values, it comes to $J_\Delta \approx 12.10^{-9} kg.m^2$. To obtain the desired circularly polarized wave, a cylindrical waveguide is fed

with two mutually perpendicular TE_{11} modes in phase quadrature. The guide radius is chosen to be $R_g = 42mm$ [35].

Using the HFSS solver of ANSYS Electronics Desktop, the device created is numerically modelled. As expected, in both models, the resulting time average torque is non-zero and maximum at the resonance frequency. The results remain of the same order of magnitude (see table I). The theoretical approach is thus reinforced.

Experimental evidence - Experimental measurements were carried out to confirm that a circular polarized wave can set a SRR in rotation.

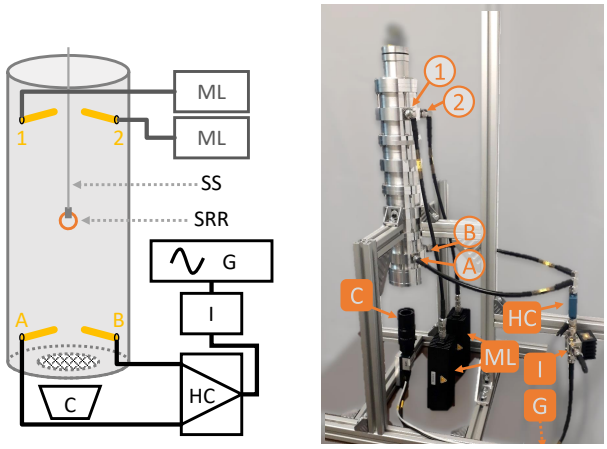

(a) Diagram of the experimental bench.

(b) Image of the experimental bench.

FIG. 2: Experimental setup. (ML : matched load ; SS : spider silk ; SRR : Split Ring Resonator ; G : radio frequency generator ; I : isolator ; HC : -3dB hybrid coupler ; A, B, 1 and 2 : matched antennas ; C : camera)

The experimental set-up is illustrated in figure 2. A generator supplies a CW microwave (here at 2.47 GHz and 200W max). This wave is split by a hybrid coupler. Each channel then carries a wave of the same amplitude (100W max) and in phase quadrature. These waves are then transferred to the guide by two matched antennas (A and B figure 2) positioned perpendicular to each other. They exit the guide via two other similarly arranged matched antennas (1 and 2 figure 2). The SRR is suspended by a spider silk, to minimize the restoring torque. The angular position of the SRR is determined by digital processing of a camera recorded video (through a microwave grid), with an estimated accuracy of $\pm 1.5°$. Two video records are provided in the supplementary material.

Several input powers were tested. For each power, at least three measurements were taken to ensure repeatability. Both rotation directions of the magnetic field have been tested (by interchanging the connections to channels A and B) to ensure that no parasitic phenomenon cause the observed movement (see supplementary materials for further details). Figures 3 and 4 illustrate the rotation of an SRR (initially at rest). In each case, repeatable behaviour is observed. In general concerns, as expected, the higher the input power, the bigger the movement. The curves are symmetrical to each other when the circular polarization is reversed. Consequently, the results show that the wave is indeed what sets the SRR in motion, as intended.

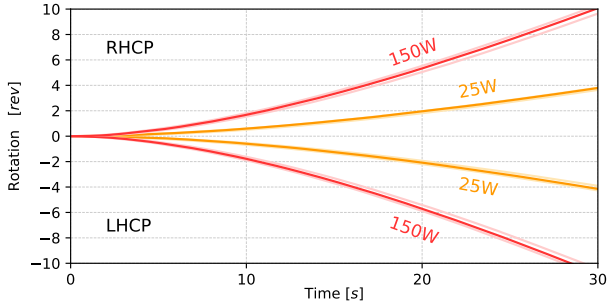

(a) Rotation.

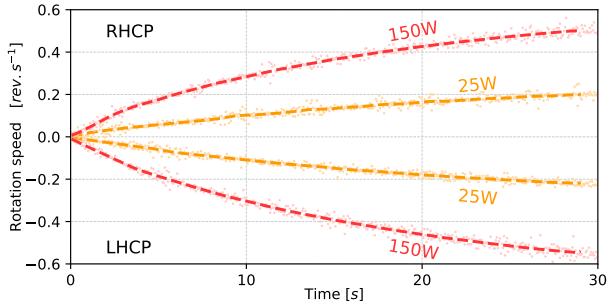

(b) Rotation speed

FIG. 3: Rotation (3a) and Rotation speed (3b) of the SRR as a function of time, at resonance frequency, for a input power of 25W and 150W, and for right and left hand circular polarization.

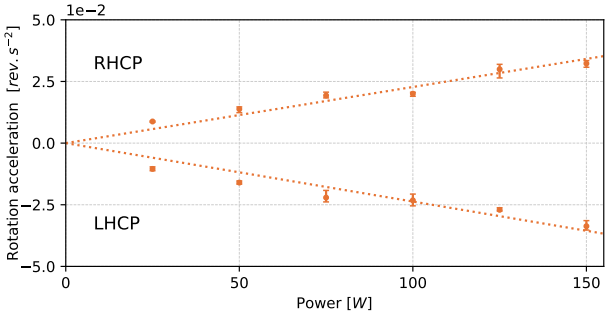

FIG. 4: Initial rotation acceleration as a function of the input power, at resonance frequency, for right and left hand circular polarization.

More specifically, figure 3a shows curves of SRR angular position as a function of time. As expected, all curves

have a parabolic shape. The rotation speed curves of the figure 3b are derived from data in figure 3a. The equation of motion, if friction is neglected (mostly at the in initial time), corresponds to a second-degree polynomial. This yields the values shown in figure 4. The linear dependence of the initial rotation acceleration on the input power is confirmed.

In terms of order of magnitude, at 150W and in less than 30 seconds, the SRR performs more than 10 revolutions and reaches rotational speeds exceeding 0.5 revolution per second.

Table I provides a comparison of the approaches presented in this letter. For the experimental approach (unlike the analytical and numerical approaches), the torque is deduced from the SRR's initial rotation acceleration (see eq (3)). The experimental set-up does not provide SRR current informations. The results obtained are of the order of magnitude anticipated.

For comparison, at 25W input power, Emile [14] reaches a rotation acceleration of his ring of around $10^{-6} rev.s^{-2}$ and thus a rotation of less than 0.5° after 30 seconds. At the same power, on the other hand, our SRR reaches a rotation acceleration of around $10^{-2} rev.s^{-2}$ and thus a rotation of around $4rev$ i.e. 1440° in 30 seconds, i.e. an experimental performance more than 10^3 times greater.

TABLE I: Comparison of analytical, numerical and experimental approaches (values obtained at resonance frequency for a generator power of 150W).

Quantites	Units	Analytical	Numerical [a]	Experimental
$\langle i_{res} \rangle$	[A]	7.4	[3.3 - 7.2]	-
$\langle \Gamma_{res} \rangle$	[nN.m]	6.0	12	2.6
$\langle \alpha_{res} \rangle$	$[rev.s^{-2}]$	8.0e-2	15e-2	3.4e-2

[a] In the numerical model, the current is not uniform along the SRR, the range of values is therefore shown.

Discussion on the experimental results - The result obtained from the experimental set-up discussed here confirms the principle explained at the start of this letter. Given the demonstrative results obtained, it was decided not to optimize the set-up. This final section discusses and justifies the choices made to obtain these results.

Firstly, the experimental bench is naturally lossy, meaning that not all input power interacts with the SRR. In addition, the mutual coupling between the two ports (A-1 and B-2, see fig.2) is significant, and implies imperfectly circular polarization. Although these phenomena have a significant impact on the torque intensity (see eq. 2), the results being fairly demonstrative, it was not decided to improve them (see supplementary materials).

Secondly, several limiting phenomena emerge as the SRR starts rotating. The SRR is subject to frictional forces (no vacuum is performed, unlike in [10, 11]). Similarly, the spider wire used was chosen for its low restoring torque. However, this torque is unlikely to be accurately measured, as its behavior is not linear with rotation, as with conventional wires [36]. Finally, since the current flowing through the SRR is of the order of a few ampere, the SRR heats up, causing its properties to evolve over time during measurement. It can be seen that rotation speed does not vary linearly with time, but rather tends towards an asymptotic value. This shows that these limiting phenomena have a non-negligible influence with increasing time. Consequently, to evaluate the rotation acceleration of the SRR, it has been decided to consider only a short initial period. The time of one revolution has been chosen. However, this choice implies an underestimation of the initial rotation acceleration.

Finally, at input powers above 150W, initial performances (rotation, speed, acceleration) lose linearity with input power (see supplementary material). It has therefore been decided to restrict the maximum power to 150W.

Conclusion - The aim of the study presented here is to set a SRR in motion by a powerful electromagnetic wave in the microwave range. A general method applied to this case leads to the use of a circularly polarized wave. Analytical, numerical and experimental studies confirm this result. This is the first experimental evidence of a SRR being set in motion by a wave at microwave frequencies, and a significant improvement (more than 10^3 times greater rotation acceleration) compared with similar experiments [14]. This high performance is due to the choice of the SRR, which is resonant and of low dimension, and therefore of low rotational inertia.

Over and above this, the experimental results confirm the validity of the models designed, and thus the understanding of the physical phenomena involved, both qualitatively and quantitatively. This opens the way to various other possibilities. As the energy received by the SRR is mainly re-radiated, resonant cavity placement should significantly increase the intensity of the torque obtained. A circular guide has been used here, but is not necessary, and a distant set in motion of the SRR, far from any material support, can be envisaged with a collimated beam. Using the current distribution of the SRR's higher resonance modes can lead to translation movement of the SRR. Experimental proof is required, however. Finally, the element studied here is the SRR. Different other elements can be envisaged.

Application of the method to other elements and periodization of these elements could ultimately lead to the design of metasurfaces dedicated to setting larger objects in motion.

Acknowledgements : The authors would like to thank DGA/AID and the company Anywaves for co-funding this work.

[1] J. Kepler, *De cometis libelli tres*, De cometis libelli tres (Typis Andreæ Apergeri, sumptibus Sebastiani Mylii bibliopolæ Augustani, 1619).

[2] L. Page, A century's progress in physics, American Journal of Science **s4-46**, 316 (1918).

[3] P. Lebedew, Untersuchungen über die druckkräfte des lichtes, Annalen der Physik **311**, 433 (1901).

[4] E. F. Nichols and G. F. Hull, A preliminary communication on the pressure of heat and light radiation, Phys. Rev. (Series I) **13**, 307 (1901).

[5] E. F. Nichols and G. F. Hull, The pressure due to radiation. (second paper.), Phys. Rev. (Series I) **17**, 26 (1903).

[6] J. H. Poynting, The wave motion of a revolving shaft, and a suggestion as to the angular momentum in a beam of circularly polarised light, Proceedings of the Royal Society of London. Series A, Containing Papers of a Mathematical and Physical Character **82**, 560 (1909).

[7] R. A. Beth, Direct detection of the angular momentum of light, Phys. Rev. **48**, 471 (1935).

[8] R. A. Beth, Mechanical detection and measurement of the angular momentum of light, Phys. Rev. **50**, 115 (1936).

[9] A. Holbourn, Angular momentum of circularly polarised light, Nature **137**, 31 (1936).

[10] P. J. Allen, A Radiation Torque Experiment, American Journal of Physics **34**, 1185 (1966).

[11] M. Kristensen, M. Beijersbergen, and J. Woerdman, Angular momentum and spin-orbit coupling for microwave photons, Optics Communications **104**, 229 (1994).

[12] G. Delannoy, O. Emile, and A. Le Floch, Direct observation of a photon spin-induced constant acceleration in macroscopic systems, Applied Physics Letters **86**, 10.1063/1.1869539 (2005), 081109.

[13] H. He, M. E. J. Friese, N. R. Heckenberg, and H. Rubinsztein-Dunlop, Direct observation of transfer of angular momentum to absorptive particles from a laser beam with a phase singularity, Phys. Rev. Lett. **75**, 826 (1995).

[14] O. Emile, C. Brousseau, J. Emile, R. Niemiec, K. Madhjoubi, and B. Thide, Electromagnetically induced torque on a large ring in the microwave range, Phys. Rev. Lett. **112**, 053902 (2014).

[15] O. Emile and J. Emile, Energy, linear momentum, and angular momentum of light: What do we measure?, Annalen der physik **530**, 1800111 (2018).

[16] A. Ashkin, Trapping of atoms by resonance radiation pressure, Phys. Rev. Lett. **40**, 729 (1978).

[17] W. D. Phillips, Nobel lecture: Laser cooling and trapping of neutral atoms, Rev. Mod. Phys. **70**, 721 (1998).

[18] D. Xu, Z. Mo, J. Jiang, H. Huang, Q. Wei, Y. Wu, X. Wang, Z. Liang, H. Yang, H. Chen, H. Huang, H. Liu, D. Deng, and L. Shui, Guiding particles along arbitrary trajectories by circular pearcey-like vortex beams, Phys. Rev. A **106**, 013509 (2022).

[19] J. Chen, C. Wan, and Q. Zhan, Engineering photonic angular momentum with structured light: a review, Advanced Photonics **3**, 064001 (2021).

[20] W. Li, X. Wang, J. Liu, S. Li, N. Li, and H. Hu, Flexible control of an ultrastable levitated orbital micro-gyroscope through orbital-translational coupling, Nanophotonics **12**, 1245 (2023).

[21] Y. Zhang, Z. Zhang, L. Liu, and Y. Zhao, Rotational doppler velocimetry of a surface at larger tilt angles, Photonics **10**, 10.3390/photonics10030341 (2023).

[22] C. R. McInnes, *Solar Sailing : Technology, Dynamics and Mission Applications* (1999).

[23] J. B. Pezent, R. Sood, A. Heaton, K. Miller, and L. Johnson, Preliminary trajectory design for nasa's solar cruiser: A technology demonstration mission, Acta Astronautica **183**, 134 (2021).

[24] K. Achouri, O. V. Céspedes, and C. Caloz, Solar "metasails" for agile optical force control, IEEE Transactions on Antennas and Propagation **67**, 6924 (2019).

[25] J. D. Jackson, *Classical Electrodynamics* (1962).

[26] D. Griffiths, *Introduction to Electrodynamics* (Prentice-Hall, 1981).

[27] M. Mansuripur, *Field, Force, Energy and Momentum in Classical Electrodynamics* (2011).

[28] J. Pendry, A. Holden, D. Robbins, and W. Stewart, Magnetism from conductors, and enhanced non-linear phenomena, Microwave Theory and Techniques, IEEE Transactions on **47**, 2075 (1999).

[29] D. R. Smith, W. J. Padilla, D. C. Vier, S. C. Nemat-Nasser, and S. Schultz, Composite medium with simultaneously negative permeability and permittivity, Phys. Rev. Lett. **84**, 4184 (2000).

[30] D. R. Smith, S. Schultz, P. Markoš, and C. M. Soukoulis, Determination of effective permittivity and permeability of metamaterials from reflection and transmission coefficients, Phys. Rev. B **65**, 195104 (2002).

[31] C. Soukoulis, M. Kafesaki, and E. Economou, Negative-index materials: New frontiers in optics, Advanced Materials **18**, 1941 (2006).

[32] A. J. Fairbanks, A. M. Darr, and A. L. Garner, A review of nonlinear transmission line system design, IEEE Access **8**, 148606 (2020).

[33] A.-N. A. Jabita, Design of singly split single ring resonator for measurement of dielectric constant of materials using resonant method (2013).

[34] J. D. Kraus, *Antennas, 2nd edition* (1988).

[35] D. Pozar, *Microwave Engineering, 4th Edition* (Wiley, 2011).

[36] O. Emile, A. L. Floch, and F. Vollrath, Time-resolved torsional relaxation of spider draglines by an optical technique, Phys. Rev. Lett. **98**, 167402 (2007).